NASA Contractor Report 187439

ICASE Report No. 90–66

ICASE

BOUNDED ENERGY STATES IN HOMOGENEOUS TURBULENT SHEAR FLOW — AN ALTERNATIVE VIEW

Peter S. Bernard
Charles G. Speziale

Contract No. NAS1–18605
October 1990

Institute for Computer Applications in Science and Engineering
NASA Langley Research Center
Hampton, Virginia 23665–5225

Operated by the Universities Space Research Association

National Aeronautics and
Space Administration

Langley Research Center
Hampton, Virginia 23665-5225

BOUNDED ENERGY STATES IN HOMOGENEOUS TURBULENT SHEAR FLOW – AN ALTERNATIVE VIEW

Peter S. Bernard
Department of Mechanical Engineering,
University of Maryland,
College Park, Maryland 20742

Charles G. Speziale*
Institute for Computer Applications in Science and Engineering,
NASA Langley Research Center,
Hampton, Virginia 23665

ABSTRACT

The equilibrium structure of homogeneous turbulent shear flow is investigated from a theoretical standpoint. Existing turbulence models, in apparent agreement with physical and numerical experiments, predict an unbounded exponential time growth of the turbulent kinetic energy and dissipation rate; only the anisotropy tensor and turbulent time scale reach a structural equilibrium. It is shown that if vortex stretching is accounted for in the dissipation rate transport equation, then there can exist equilibrium solutions, with bounded energy states, where the turbulence production is balanced by its dissipation. Illustrative calculations are presented for a $k - \epsilon$ model modified to account for vortex stretching. The calculations indicate an initial exponential time growth of the turbulent kinetic energy and dissipation rate for elapsed times that are as large as those considered in any of the previously conducted physical or numerical experiments on homogeneous shear flow. However, vortex stretching eventually takes over and forces a production-equals-dissipation equilibrium with bounded energy states. The validity of this result is further supported by an independent theoretical argument. It is concluded that the generally accepted structural equilibrium for homogeneous shear flow with unbounded component energies is in need of re-examination.

*Research supported by the National Aeronautics and Space Administration under NASA Contract No. NAS1-18605 while the author was in residence at the Institute for Computer Applications in Science and Engineering (ICASE), NASA Langley Research Center, Hampton, VA 23665-5225.

1. INTRODUCTION

Homogeneous turbulent shear flow has been the subject of a variety of experimental, computational and theoretical studies during the past four decades. The popularity of this flow lies in the fact that it accounts for an important physical effect – the alteration of the turbulence structure by shear – in a simplified setting unencumbered by such complications as rigid boundaries and mean turbulent diffusion. Von Karman[1] first proposed the problem of homogeneous shear flow which gave rise to some mathematical studies during the 1950's (c.f. Townsend[2] and Hinze[3] for a review). It is a difficult flow to simulate experimentally and the first tangible suggestion for its generation was put forth by Corrsin[4]. The first successful experimental realization of homogeneous shear flow in the laboratory was achieved by Rose[5] and was followed by a series of landmark experiments by Corrsin and co-workers[6–8]. More recently, Tavoularis and Karnik[9] and Rohr et al.[10] performed more exhaustive measurements of homogeneous shear flow shedding new light on its basic structure.

With the dramatic increase in computer capacity achieved by the late 1970's, direct numerical simulations of homogeneous turbulent flows became possible. Rogallo[11] was the first to conduct a direct simulation of homogeneous shear flow; the results that he obtained were well within the range of the experiments of Tavoularis and Corrsin[8]. Subsequently, Bardina et al.[12] performed a coarse-grid large-eddy simulation of homogeneous shear flow and Rogers, Moin and Reynolds[13] conducted fine-grid $128 \times 128 \times 128$ direct simulations which further clarified its structure.

The early experiments of Rose[5] and Champagne, et al.[6], which were conducted for relatively weak shear rates and small elapsed times, seemed to indicate that the Reynolds stresses (and, hence, the turbulent kinetic energy) asymptoted to equilibrium values. This asymptotic state is consistent with the production-equals-dissipation equilibrium that had been hypothesized by Townsend[2] several years earlier. However, the integral length scales were still growing monotonically at the end of the Rose[5] and Champagne et al.[6] experiments suggesting the strong possibility that an asymptotic state had not yet been reached. Subsequent physical experiments[8–10] and direct numerical simulations[11–13], conducted for stronger shear rates and larger elapsed times, confirmed this. These physical and numerical experiments, along with alternative theoretical analyses (see Rogallo[11] and Tavoularis[14]), have led to the following widely accepted physical picture of homogeneous shear flow:

(1) the turbulent kinetic energy k and dissipation rate ϵ grow exponentially in time at the same rate,

(2) the anisotropy tensor b_{ij} and the dimensionless turbulent time scale Sk/ϵ reach equilibrium values that are relatively independent of the initial conditions and the shear rate S.

It should be noted that Speziale and MacGiolla Mhuiris[15] have recently shown that virtually all of the commonly used two-equation turbulence models and second-order closures are consistent with this hypothetical picture of homogeneous shear flow.

An alternative physical picture of homogeneous shear flow is presented in this paper which is consistent with the previously conducted physical and numerical experiments, yet at the same time is more intuitively satisfying in that it excludes the occurrence of unbounded energy growth. In particular, it will be shown that when vortex stretching is accounted for in the dissipation rate transport equation, a production-equals-dissipation equilibrium results in which the turbulent kinetic energy and dissipation rate eventually asymptote to bounded values. Illustrative calculations are presented for a $k-\epsilon$ model suitably modified to account for vortex stretching. Consistent with physical and numerical experiments, these calculations indicate an exponential time growth of the turbulent kinetic energy and dissipation rate for $St < 30$. This is the largest elapsed time considered in any of these previous experimental studies. However, for $St > 30$, vortex stretching eventually takes over causing the system to saturate and attain an equilibrium structure with bounded kinetic energy and dissipation. In the sections to follow, a detailed case is made to establish that this alternative equilibrium structure of homogeneous shear flow is a serious possibility that could have important implications for turbulence modeling at high Reynolds numbers.

2. THEORETICAL BACKGROUND

We will consider the incompressible and isothermal turbulent flow of a viscous fluid. The governing field equations are the Navier-Stokes and continuity equations given by

$$\frac{\partial v_i}{\partial t} + v_j \frac{\partial v_i}{\partial x_j} = -\frac{\partial P}{\partial x_i} + \nu \nabla^2 v_i \tag{1}$$

$$\frac{\partial v_i}{\partial x_i} = 0 \tag{2}$$

where v_i is the velocity vector, P is the modified pressure and ν is the kinematic viscosity of the fluid. As in the usual treatments of turbulence, the velocity and pressure will be decomposed into ensemble mean and fluctuating parts, respectively:

$$v_i = \overline{v_i} + u_i, \quad P = \overline{P} + p. \tag{3}$$

For homogeneous shear flow, the mean velocity-gradient tensor takes the form

$$\frac{\partial \overline{v_i}}{\partial x_j} = \begin{pmatrix} 0 & S & 0 \\ 0 & 0 & 0 \\ 0 & 0 & 0 \end{pmatrix}. \tag{4}$$

In direct numerical simulations of homogeneous shear flow, an initially isotropic turbulence is subjected to the constant shear rate S and its time evolution is then computed. In laboratory experiments, an initially decaying isotropic turbulence, created downstream of a grid, is subjected to a uniform shear rate as it evolves spatially. The two problems are related, in an *approximate* sense, by the Galilean transformation

$$x = x_o + U_c t \tag{5}$$

where U_c is a characteristic mean velocity that is typically taken to be the centerline mean velocity of the uniform shear [hence, dimensionless time $St \equiv S(x - x_o)/U_c$]. For the remainder of this paper, we will only consider the temporally evolving version of homogeneous shear flow, since it is the only version of this problem that is *exactly* homogeneous.

In any homogeneous turbulent flow, the exact transport equations for the turbulent kinetic energy $k \equiv \frac{1}{2}\overline{u_i u_i}$ and dissipation rate $\epsilon \equiv \nu \overline{\frac{\partial u_i}{\partial x_j}\frac{\partial u_i}{\partial x_j}}$ take the form[16]

$$\dot{k} = \mathcal{P} - \epsilon \tag{6}$$

$$\dot{\epsilon} = \mathcal{P}_{\epsilon S} + \mathcal{P}_{\epsilon V} - \Phi_\epsilon \tag{7}$$

where

$$\mathcal{P} = -\tau_{ij}\frac{\partial \overline{v_i}}{\partial x_j}, \quad \mathcal{P}_{\epsilon S} = 2\nu\, \overline{\omega_i \omega_j}\frac{\partial \overline{v_i}}{\partial x_j}, \tag{8}$$

$$\mathcal{P}_{\epsilon V} = 2\nu\, \overline{\omega_i \omega_j \frac{\partial u_i}{\partial x_j}}, \quad \Phi_\epsilon = 2\nu^2 \overline{\frac{\partial \omega_i}{\partial x_j}\frac{\partial \omega_i}{\partial x_j}}, \tag{9}$$

are, respectively, the production of turbulent kinetic energy, the production of dissipation by mean strains, the production of dissipation by vortex stretching, and the destruction

of dissipation. In (8) - (9), $\tau_{ij} \equiv \overline{u_i u_j}$ is the Reynolds stress tensor and $\omega \equiv \nabla \times \mathbf{u}$ is the fluctuating vorticity vector. At this stage, we introduce the anisotropy tensor b_{ij} defined as

$$b_{ij} = \frac{(\tau_{ij} - \frac{2}{3}k\delta_{ij})}{2k} \tag{10}$$

which will be useful in the analysis to follow.

If we non-dimensionalize the turbulent kinetic energy, dissipation rate, and time as follows:

$$k^* \equiv \frac{k}{k_o}, \quad \epsilon^* \equiv \frac{\epsilon}{\epsilon_o}, \quad t^* \equiv St,$$

where k_o and ϵ_o denote initial values, then the exact transport equation (6) for k can be rewritten in the dimensionless form

$$\dot{k^*} = 2\left(\frac{\epsilon}{\mathcal{P}} - 1\right) b_{12} k^* \tag{11}$$

since $\mathcal{P} = -\tau_{12} S$ in homogeneous shear flow. It should be noted that the ratio of production to dissipation $\mathcal{P}/\epsilon$ can be related to b_{12} through the identity

$$\frac{\mathcal{P}}{\epsilon} = -2b_{12}\frac{Sk}{\epsilon}. \tag{12}$$

Consequently, if any two of the quantities $\mathcal{P}/\epsilon$, b_{12} and Sk/ϵ are known, the remaining one can be computed using (12). Furthermore, since for homogeneous shear flow $\mathcal{P}/\epsilon > 0$ and $Sk/\epsilon > 0$, it follows from (12) that $b_{12} < 0$. Physical and numerical experiments have tended to indicate that b_{12} and Sk/ϵ reach equilibrium values that are relatively independent of the initial conditions. More specifically, these experiments suggest the results

$$\left(\frac{Sk}{\epsilon}\right)_\infty \approx 6.0, \quad (b_{12})_\infty \approx -0.15, \quad \left(\frac{\mathcal{P}}{\epsilon}\right)_\infty \approx 1.8 \tag{13}$$

where $(\ .\ )_\infty$ is the equilibrium value obtained in the limit as $t \to \infty$. From (11) and (12) it follows that for $t^* \gg 1$

$$k^* \sim \exp(\lambda t^*) \tag{14}$$

where the growth rate λ is given by

$$\lambda = 2\left[\left(\frac{\epsilon}{\mathcal{P}}\right)_\infty - 1\right](b_{12})_\infty \approx 0.14. \tag{15}$$

Equations (13) and (14) then imply that for $t^* \gg 1$

$$\epsilon^* \sim \exp(\lambda t^*) \tag{16}$$

since, if k grows exponentially and Sk/ϵ equilibrates, then ϵ must grow exponentially at the same rate. This constitutes an alternate derivation of the Tavoularis[14] asymptotic law of exponential growth in shear flow. The wealth of experimental data on homogeneous shear flow collected over the past two decades appears to be in agreement with this hypothetical physical picture. This is evidenced by Figure 1 containing several sets of measured k data versus non-dimensional time that was recently compiled by Rohr, et al.[10].

In order for this structural equilibrium – with an unbounded exponential time growth of k and ϵ – to be valid, the higher order correlations in the dissipation rate transport equation (7) must satisfy certain consistency conditions. When non-dimensionalized, (7) takes the form

$$\dot{\epsilon^*} = \left(\frac{2\overline{\omega_1\omega_2}}{\overline{\omega_k\omega_k}} + \frac{2\overline{\omega_i\omega_j\frac{\partial u_i}{\partial x_j}}}{(\overline{\omega_k\omega_k})^{\frac{3}{2}}} \frac{\epsilon}{Sk}\sqrt{R_t} - \frac{2\nu}{S}\frac{\overline{\frac{\partial\omega_i}{\partial x_j}\frac{\partial\omega_i}{\partial x_j}}}{\overline{\omega_k\omega_k}} \right) \epsilon^* \tag{17}$$

where $R_t \equiv k^2/\nu\epsilon$ is the turbulence Reynolds number. In deriving (17), we have made use of the fact that $\epsilon \equiv \nu\overline{\omega_i\omega_i}$ since the turbulence is homogeneous. The first of the three correlations

$$\frac{\overline{\omega_1\omega_2}}{\overline{\omega_k\omega_k}}, \quad \frac{\overline{\omega_i\omega_j\frac{\partial u_i}{\partial x_j}}}{(\overline{\omega_k\omega_k})^{\frac{3}{2}}}, \quad \frac{2\nu\overline{\frac{\partial\omega_i}{\partial x_j}\frac{\partial\omega_i}{\partial x_j}}}{\overline{\omega_k\omega_k}}$$

appearing in (17) is bounded by the Schwarz inequality. Direct numerical simulations of Rogers[17] for homogeneous shear flow, as shown in Figure 2, indicate that the second of these correlations (which is proportional to the skewness S_K in an isotropic turbulence) asymptotes fairly quickly to an apparent equilibrium value of 0.1. Hence, assuming the equilibration of ϵ/Sk, it follows that in order to recover the exponential growth law (16) for $t^* \gg 1$, we must have the third of these correlations behave as

$$\nu\frac{\overline{\frac{\partial\omega_i}{\partial x_j}\frac{\partial\omega_i}{\partial x_j}}}{\overline{\omega_k\omega_k}} \sim \sqrt{R_t} \sim \exp(\frac{1}{2}\lambda t). \tag{18}$$

While (18) may appear to be consistent with the traditionally accepted scaling laws for equilibrium turbulent flows[16], it is a somewhat questionable possibility for homogeneous shear flow where one might expect this correlation to equilibrate. In particular, this term represents the ratio of the destruction of enstrophy to the enstrophy. The analogous quantity for the turbulent kinetic energy – namely, the ratio of the "destruction of turbulent kinetic energy" (ϵ) to the turbulent kinetic energy (k) – does reach an equilibrium value for large times. Direct numerical simulations of homogeneous shear flow do

not support (18), although the issue is still far from settled (see Figure 3 obtained from Rogers[17], which is *not* suggestive of a $\sqrt{R_t}$ growth).

We will now consider possible alternative equilibrium states for homogeneous shear flow. There are two such possibilities:

(1) an alternative structural equilibrium where $(\epsilon/Sk)_\infty = 0$, or

(2) a production-equals-dissipation equilibrium with bounded energy states (i.e., with $k_\infty < \infty$ and $\epsilon_\infty < \infty$).

The former structural equilibrium where $(\epsilon/Sk)_\infty = 0$ has been shown by Speziale and MacGiolla Mhuiris[15] to be primarily associated with solutions for k and ϵ that undergo a power law growth with time (i.e., for $St \gg 1, k \sim t^\alpha, \epsilon \sim t^\beta$ where $\alpha > \beta$). However, these solutions are largely unstable within the context of Reynolds stress transport models. Furthermore, at the end of all of the previously conducted physical and numerical experiments on homogeneous shear flow, ϵ/Sk either appeared to equilibrate to a non-zero value or continued to grow – results that are not suggestive of an equilibrium state where $(\epsilon/Sk)_\infty = 0$. Hence, we feel that this alternative equilibrium structure is not a strong possibility.

The second possibility – namely, the production-equals-dissipation equilibrium – appears to contradict the physical and numerical experiments which indicate that the turbulent kinetic energy and dissipation rate are still growing at the end of the experiments (i.e., for elapsed times St as large as 28). However, a production-equals-dissipation equilibrium wherein

$$\mathcal{P}_\infty = \epsilon_\infty \tag{19}$$

$$\Phi_{\epsilon_\infty} = \mathcal{P}_{\epsilon_{S\infty}} + \mathcal{P}_{\epsilon_{V\infty}} \tag{20}$$

(with bounded values for $k_\infty, \epsilon_\infty$ and R_{t_∞}) is consistent with the ensemble averaged Navier-Stokes equations. In the following sections, it will be shown that when the vortex stretching term is accounted for in the dissipation rate transport equation, then this production-equals-dissipation equilibrium (with an early exponential time growth of k and ϵ for $St < 30$) becomes a serious possibility.

3. THE DISSIPATION RATE TRANSPORT EQUATION WITH VORTEX STRETCHING

Batchelor and Townsend[18] have shown that the transient behavior of the enstrophy

$\omega^2 \equiv \overline{\omega_i \omega_i}$ in isotropic turbulence is governed by the equation

$$\frac{d\omega^2}{dt} = \frac{7}{3\sqrt{15}}\omega^3 S_K - \frac{14}{3\sqrt{15}}\omega^3 \frac{G}{R_\lambda} \tag{21}$$

where

$$S_K = -\frac{\overline{\left(\frac{\partial u}{\partial x}\right)^3}}{\left[\overline{\left(\frac{\partial u}{\partial x}\right)^2}\right]^{\frac{3}{2}}} \tag{22}$$

is the skewness of the probability density function of $\frac{\partial u}{\partial x}$ defined with a negative sign to make it positive definite. In (21), $R_\lambda \equiv u_{rms}\lambda/\nu$ is the turbulence Reynolds number based on the Taylor microscale and G is a function defined by

$$G \equiv \lambda^4 f_o^{iv}. \tag{23}$$

Here, u_{rms} is the root-mean-square of the velocity fluctuation component u, λ is the Taylor microscale derived from the two point longitudinal velocity correlation function $f(r)$, and f_o^{iv} is the fourth derivative of $f(r)$ evaluated at $r = 0$. The first term on the right-hand side of (21) accounts for the effect of vortex stretching and is positive definite, while the second term is always negative and leads to the destruction of enstrophy.

Equation (21) may be converted into a transport equation for ϵ through use of the identity

$$\epsilon = \nu\omega^2, \tag{24}$$

which is valid for any homogeneous turbulence. Since the defining equation for the microscale may be conveniently written as

$$\omega^2 = \frac{10k}{\lambda^2}, \tag{25}$$

it follows that (21) can be converted to the equation

$$\dot{\epsilon} = \frac{7}{3\sqrt{15}}\frac{S_K}{\sqrt{\nu}}\epsilon^{\frac{3}{2}} - \frac{7}{15}G\frac{\epsilon^2}{k}. \tag{26}$$

Once values are obtained for S_K and G, (26) may be solved together with the kinetic energy equation

$$\dot{k} = -\epsilon \tag{27}$$

yielding a solution for isotropic decay.

Batchelor and Townsend[18] showed that if G has the form

$$G = \frac{30}{7} + \frac{1}{2} R_\lambda S_K, \tag{28}$$

then the solution of (26) - (27) is compatible with their experimental data showing a power law decay of the kinetic energy, with an exponent of approximately one, for the case of moderately large values of R_λ. More precisely, the substitution of (28) into (26) yields the equation

$$\dot{\epsilon} = -2\frac{\epsilon^2}{k}, \tag{29}$$

which, when combined with (27), gives rise to the exact solution

$$k = k_o \left(1 + \frac{\epsilon_o t}{k_o}\right)^{-1}$$

for isotropic decay (i.e., a power law decay where $k \sim t^{-1}$). Apart from the specific value of the numerical coefficient on the right-hand side of (29), which is more commonly set to a value ranging from 1.83 - 1.92 to reflect more recent decay data[19] suggesting that $k \sim t^{-1.1}$ or $k \sim t^{-1.2}$, the form of (29) is one which forms a cornerstone for the standard modeled ϵ transport equation that is widely used in turbulence models.

In the approach of Batchelor and Townsend, the choice of G given by (28) forces the vortex stretching term in (26) to be exactly subsumed by the action of the destruction of enstrophy term. This assumption, as has been noted above, guarantees compatibility with their isotropic decay data. However, it seems highly unlikely that two terms which represent distinct physical processes would *exactly* counterbalance each other, especially since the destruction of enstrophy term vanishes in the limit of zero viscosity whereas the vortex stretching term does not. In fact, the survival of the vortex stretching term in the limit of zero viscosity (i.e., the limit as $R_t \to \infty$) is crucial for the prediction of enstrophy blow-up – a property of solutions of the Euler equation (see Lesieur[20]). This can be seen by setting ν equal to zero in (21) which yields the equation

$$\frac{d\omega^2}{dt} = \frac{7}{3\sqrt{15}} \omega^3 S_K^{(0)} \tag{30}$$

where $S_K^{(0)}$ is the zero-viscosity skewness. For constant $S_K^{(0)} > 0$, (30) predicts that the enstrophy blows up at the critical time

$$t_c = \frac{6\sqrt{15}}{7\omega_o} \frac{1}{S_K^{(0)}}$$

where ω_o^2 is the initial enstrophy. Although EDQNM supports this result, a finite-time enstrophy blow-up has not been seen in direct numerical simulations of the Euler equation (see Lesieur[20] and Pumir and Siggia[21]). This means that either $S_K^{(0)}$ is a very small constant or a monotonically decreasing function of time (in the former case the enstrophy would blow-up at $t_c \gg \omega_o$ whereas in the latter case it would just grow monotonically without bound as $t \to \infty$). While this issue has not been fully resolved, one thing is clear: $S_K^{(0)}$ is *not* identically zero. If $S_K^{(0)} = 0$, then (30) yields the erroneous prediction

$$\omega^2 = constant$$

which is not supported by direct numerical simulations or theoretical analyses of the Euler equation (these indicate that the enstrophy grows dramatically due to vortex stretching).

The standard modeled dissipation rate equation (29) reduces to

$$\frac{d\omega^2}{dt} = 0$$

in the limit of zero viscosity and, hence, incorrectly predicts (in agreement with the $S_K^{(0)} = 0$ case) that the enstrophy is conserved. It is a simple matter to show that (28) is *equivalent* to the alternative scaling

$$G \sim constant, \quad S_K \sim R_\lambda^{-1} \tag{31}$$

in the ϵ transport equation for $R_\lambda \gg 1$. The scaling of G in (31) can be obtained by making the assumption that

$$\frac{2\nu \overline{\frac{\partial \omega_i}{\partial x_j}\frac{\partial \omega_i}{\partial x_j}}}{\overline{\omega_k \omega_k}} \propto \frac{\epsilon}{k}$$

(namely, by the assumption that the time scale of the destruction of dissipation is proportional to the time scale of the destruction of turbulent kinetic energy). While this scaling for G is quite reasonable, the scaling of S_K in (31) is not acceptable since it gives rise to a vanishing skewness in the limit of infinite turbulence Reynolds numbers (or zero viscosity). Hence, we will maintain the first part of equation (31) but we will *not* set $S_K^{(0)}$ to zero. A Taylor series expansion of S_K in the variable R_λ^{-1} yields

$$S_K = S_K^{(0)} + S_K^{\prime(0)} R_\lambda^{-1} \; + \; ... \tag{32}$$

where $S_K^{\prime(0)} = [\partial S_K / \partial R_\lambda^{-1}]_{R_\lambda^{-1}=0}$. By substituting the first part of (31) and (32) into (26), we obtain the alternative modeled dissipation rate equation

$$\dot{\epsilon} = \frac{7}{3\sqrt{15}} \frac{S_K^{(0)}}{\sqrt{\nu}} \epsilon^{\frac{3}{2}} - C_{\epsilon_2} \frac{\epsilon^2}{k} \tag{33}$$

where C_{ϵ_2} can be taken to be a constant for $R_\lambda \gg 1$ (in deriving (33) we have made use of the fact that $R_\lambda^{-1} \sim R_t^{-1/2}$ and that $\epsilon^{3/2}/\sqrt{\nu} \equiv R_t^{1/2}\epsilon^2/k$). In the limit as $S_K^{(0)} \to 0$, the traditional modeled transport equation for ϵ is recovered. We take $C_{\epsilon_2} = 1.90$, rather than 2.0, since this value yields a power law decay in isotropic turbulence where $k \sim t^{-1.1}$ – a value that is more in the range of the most recent experiments[19]. As alluded to earlier, since direct numerical simulations of the Euler equation have failed to yield finite time enstrophy blow-up, the zero viscosity skewness $S_K^{(0)}$ is likely to be small. Lagrangian based simulations of the Euler equation conducted recently by Girimaji and Pope[22] yielded values for $S_K^{(0)}$ that were of the order of 10^{-2}. Hence, for all of the illustrative calculations of this paper, we will set

$$S_K^{(0)} = 0.01$$

for simplicity (or course, $S_K^{(0)}$ could more generally be a monotonically decreasing function of time).

In figure 4(a), a solution of (33) for isotropic decay is given for $R_{t_o} = 300$ (it should be noted that the new ϵ-transport equation with vortex stretching depends on R_{t_o} whereas the more traditional model does not). It is clear that for this value of R_{t_o}, vortex stretching has little effect on the solution. In fact, for $R_{t_o} < 10,000$ – which includes virtually all of the physical and numerical experiments that have been conducted on isotropic turbulence – the differences are not major. It is only for extremely high turbulence Reynolds numbers (i.e., for $R_{t_o} > 100,000$) that vortex stretching makes a major difference. For example, for $R_{t_o} = 10^6$, the enstrophy predicted by this new model exhibits a dramatic early time growth which is reminiscent of the prelude to enstrophy blow-up predicted by EDQNM for large values of R_{t_o} (see figure 4(b) and figure VI - 4 of Lesieur[20]).

For anisotropic homogeneous turbulent flows, (33) can be generalized to the form

$$\dot{\epsilon} = \mathcal{P}_{\epsilon_S} + \frac{7}{3\sqrt{15}}\frac{S_K^{(0)}}{\sqrt{\nu}}\epsilon^{\frac{3}{2}} - C_{\epsilon_2}\frac{\epsilon^2}{k}, \tag{34}$$

where $\mathcal{P}_{\epsilon_S}$ is the production of dissipation by mean strains given by (8). In order to achieve closure, a model for $\mathcal{P}_{\epsilon_S}$ is needed. For simple homogeneously strained turbulent flows, it can be assumed that

$$\mathcal{P}_{\epsilon_S} \propto \mathcal{P} \tag{35}$$

which, after invoking elementary dimensional analysis, yields the model

$$\dot{\epsilon} = C_{\epsilon_1}\frac{\epsilon}{k}\mathcal{P} + \frac{7}{3\sqrt{15}}\frac{S_K^{(0)}}{\sqrt{\nu}}\epsilon^{\frac{3}{2}} - C_{\epsilon_2}\frac{\epsilon^2}{k}, \tag{36}$$

where C_{ϵ_1} is a dimensionless constant. The model for $\mathcal{P}_{\epsilon_S}$ in (36) has been used in the $k-\epsilon$ model of turbulence as well as in more complex second-order closures. Its success is largely tied to the fact that it constitutes a good approximation for plane shear flows[13,15] – the type of flow being considered in this study. For practical calculations, C_{ϵ_1} can be taken to be 1.45 (a value obtained from equilibrium shear flows). In the next section, we will apply this model to homogeneous shear flow.

4. ILLUSTRATIVE CALCULATIONS

In order to illustrate the effect of vortex stretching on homogeneous shear flow, we will present the results of calculations with a $k-\epsilon$ model for which the Reynolds stress tensor is modeled by

$$\tau_{ij} = -C_\mu \frac{k^2}{\epsilon}\left(\frac{\partial \overline{v}_i}{\partial x_j} + \frac{\partial \overline{v}_j}{\partial x_i}\right), \tag{37}$$

where $C_\mu = 0.09$ is a dimensionless constant. While the $k-\epsilon$ model is somewhat simplistic since it is based on an eddy viscosity, it was recently shown by Speziale and MacGiolla Mhuiris[15] that this model is topologically equivalent to the more complex second-order closure models for homogeneous shear flow (the deficiencies in the $k-\epsilon$ model only become pronounced when there are combinations of shear and rotation or multi-dimensional strains). Hence, (37) will suffice to illustrate the qualitative changes induced when the effect of vortex stretching on the dissipation rate is accounted for. Equation (37) will be solved in conjunction with equations (6) and (36). The standard $k-\epsilon$ model is recovered in the limit as $S_K^{(0)} \to 0$.

For homogeneous shear flow, the $k-\epsilon$ model with vortex stretching yields the transport equations

$$\dot{k} = C_\mu \frac{k^2}{\epsilon} S^2 - \epsilon \tag{38}$$

and

$$\dot{\epsilon} = C_{\epsilon_1} C_\mu k S^2 + \frac{7}{3\sqrt{15}} \frac{S_K^{(0)}}{\sqrt{\nu}} \epsilon^{\frac{3}{2}} - C_{\epsilon_2} \frac{\epsilon^2}{k} \tag{39}$$

which are obtained by substituting (4) into (6), (36) and (37).

For all non-zero values of $S_K^{(0)}$ it is a simple matter to show that the solution to (38) and (39) converges to an equilibrium state, with bounded energies. The equilibrium values may be found by setting the right-hand-sides of (38)-(39) to zero, yielding the

results

$$\frac{k_\infty}{k_o} = \frac{135}{49}\frac{\sqrt{C_\mu}(C_{\epsilon_2} - C_{\epsilon_1})^2}{S_K^{(0)^2} R_{t_o}}\frac{Sk_o}{\epsilon_o} \tag{40}$$

and

$$\frac{\epsilon_\infty}{\epsilon_o} = \frac{135}{49}\frac{C_\mu(C_{\epsilon_2} - C_{\epsilon_1})^2}{S_K^{(0)^2} R_{t_o}}\left(\frac{Sk_o}{\epsilon_o}\right)^2. \tag{41}$$

These relations clearly indicate that k_∞/k_o and $\epsilon_\infty/\epsilon_o$ have a $S_K^{(0)^{-2}}$ dependence so that the standard $k-\epsilon$ model prediction of an unbounded growth of k and ϵ is easily recovered in the limit as $S_K^{(0)} \to 0$.

Using (40) and (41) the following additional equilibrium values are also obtained for this $k-\epsilon$ model with vortex stretching:

$$\left(\frac{Sk}{\epsilon}\right)_\infty = \frac{1}{\sqrt{C_\mu}}, \tag{42}$$

$$\left(\frac{-\overline{uv}}{k}\right)_\infty = \sqrt{C_\mu} \tag{43}$$

and

$$R_{t_\infty} = \frac{135}{49}\frac{(C_{\epsilon_2} - C_{\epsilon_1})^2}{S_K^{(0)^2}}. \tag{44}$$

These results (which are independent of the initial conditions) differ from the values of $(Sk/\epsilon)_\infty = \sqrt{\alpha/C_\mu}$, $(-\overline{uv}/k)_\infty = \sqrt{\alpha C_\mu}$, and $R_{t_\infty} = \infty$ obtained from the standard $k-\epsilon$ model where $\alpha \equiv (C_{\epsilon_2} - 1)/(C_{\epsilon_1} - 1) \approx 2$. The mechanism by which the presence of the vortex stretching term has the effect of creating bounded long time solutions lies in its enhancement of the growth rate of ϵ. Evidently, this increase in the growth rate of ϵ is accompanied by a simultaneous reduction in the production of k, thus forcing a production-equals-dissipation equilibrium. In alternative terms, vortex stretching – which becomes more pronounced at high turbulence Reynolds numbers since it scales as $\sqrt{R_t}$ – eventually causes homogeneous shear flow to undergo a saturation to an equilibrium state with bounded component energies (the values of which are set by the shear rate and the viscosity).

We will now show that the $k-\epsilon$ model with vortex stretching yields temporal evolutions of the turbulence fields for $St < 30$ that are in good qualitative agreement with previously conducted physical and numerical experiments. When non-dimensionalized, (38) - (39) take the form

$$\dot{k^*} = C_\mu \frac{Sk_o}{\epsilon_o}\frac{k^{*^2}}{\epsilon^*} - \frac{\epsilon_o}{Sk_o}\epsilon^* \tag{45}$$

$$\dot{\epsilon}^* = C_{\epsilon_1} C_\mu \frac{Sk_o}{\epsilon_o} k^* + \frac{7}{3\sqrt{15}} S_K^{(0)} \frac{\epsilon_o}{Sk_o} \sqrt{R_{t_o}} \epsilon^{*\frac{3}{2}} - C_{\epsilon_2} \frac{\epsilon_o}{Sk_o} \frac{\epsilon^{*2}}{k^*} \tag{46}$$

where again we have $C_\mu = 0.09, C_{\epsilon_1} = 1.45, C_{\epsilon_2} = 1.90$ and $S_K^{(0)} = 0.01$ (the standard $k - \epsilon$ model is obtained by setting $S_K^{(0)} = 0$). The initial conditions, which correspond to an isotropic turbulence, are taken to be $\epsilon_o/Sk_o = 0.296$ and $R_{t_o} = 300$. These are the approximate initial conditions of the large-eddy simulations of Bardina et al.[12] which will allow us to make some direct comparisons between the model and the simulations.

Figures 5(a) and 6(a) display the short time solutions for k^* and ϵ^* compared to the large eddy simulation data. The solutions with non-zero vortex stretching are seen to display short term exponential growth in a manner very similar to that in the standard $k - \epsilon$ closure. The effect of the vortex stretching term is to reduce the growth rate of k^* and ϵ^*, though initially there is a slight increase in the magnitude of ϵ^*. A view of these solutions over a much longer time interval, as displayed in Figures 5(b) and 6(b), reveals the dramatic effect that the vortex stretching term ultimately has on the long term growth of k^* and ϵ^*. It is seen that with the vortex stretching effect included, the initial exponential growth rates are eventually suppressed, so that by $St \approx 40$, k^* and ϵ^* asymptote to bounded equilibrium values.

Figures 7 and 8 show the short and long time behavior of the dimensionless ratios Sk/ϵ and $-\overline{uv}/k$ for the solutions obtained with and without vortex stretching. The curves in Figures 7(a) and 8(a) give the impression that an equilibrium state for these quantities may have been achieved by the time $St \approx 10$. However, the long time solutions reveal that, in the case where vortex stretching effects are included, only a local maximum is reached – further developments must occur before a true equilibrium is achieved. This suggests that the apparent convergence of quantities such as Sk/ϵ seen in numerical and experimental studies, may not signify that a final equilibrium state has resulted (i.e., it may only be a local maximum). The behavior of Sk/ϵ shown in Figure 7(b) with vortex stretching present is remarkably consistent with the direct simulations of Rogers et al.[13] shown in Figure 9 (i.e., the tails in the computations of Rogers et al.[13] may indicate that an equilibrium state has not been reached).

Figure 10 provides a plot of the long time behavior of the computed turbulence Reynolds number. It achieves an equilibrium value of approximately 5600, which is more than eighteen times its initial value. The most significant effect of the vortex stretching term on k^* and ϵ^*, as seen in Figures 5(b) and 6(b), occurs for $R_t > 4000$. This confirms the belief that vortex stretching is mostly a phenomenon associated with high turbulence

Reynolds numbers. Finally, some indication of the sensitivity of the computed solutions to the skewness $S_K^{(0)}$ appearing in the vortex stretching term is shown in Figure 11. This contains the time evolution of k^* for a range of values of $S_K^{(0)}$; as expected, k_∞^* increases with decreasing values of $S_K^{(0)}$. Figure 12 shows the effect on k^* of a change in the initial values of ϵ_o/Sk. As would be expected on physical grounds, an increase in the dimensionless shear rate leads to a higher equilibrium value for the turbulent kinetic energy.

5. CONCLUSIONS

An alternative view concerning the equilibrium structure of homogeneous turbulent shear flow has been presented based on the inclusion of the effect of vortex stretching. It was shown that the presence of just a small amount of vortex stretching can ultimately lead to a production-equals-dissipation equilibrium with bounded energy states. For elapsed times $St < 30$ – which includes the largest values of St considered in any of the previously conducted physical and numerical experiments – the introduction of a small vortex stretching term into the standard modeled dissipation rate transport equation still yields an exponentially growing kinetic energy and dissipation for early times. However, since this vortex stretching term scales as $\sqrt{R_t}$, it eventually becomes dominant, causing a saturation of the system to an equilibrium state with bounded turbulent kinetic energy and dissipation. Although this alternative physical picture of homogeneous shear flow is contrary to the commonly accepted asymptotic laws, for which an unbounded exponential time growth of k and ϵ is postulated, it is a real possibility that needs to be seriously considered in the future. New physical and numerical experiments, for larger elapsed times St, could shed more light on the issue. The recent experiments of Tavoularis and Karnik[9], which were conducted up to $St = 28$, did show some tendency of the integral length scales to level off – a feature which, if more solidly established, would be supportive of the existence of a production-equals-dissipation equilibrium. However, it is possible for the kinetic energy and dissipation rate to equilibrate while the integral length scales grow without bound (perhaps this is the more likely possibility since the flow field is infinite).

Finally, some comments should be made concerning the implications that the results of this paper have on turbulence modeling. Since all of the commonly used two-equation models and second-order closures based on the turbulent dissipation rate neglect vortex

stretching, they predict an unbounded exponential time growth of k and ϵ in homogeneous shear flow. This type of behavior has been shown to cause problems in the calculation of certain inhomogeneous turbulent flows. The singularity in plane stagnation point turbulent flow represents a prime example[23]. Hence, if it is ultimately justified, the alteration of turbulence models to yield a production-equals-dissipation equilibrium in homogeneous shear flow via vortex stretching could make their behavior more robust in other turbulent flows. A full resolution of this issue is only likely to come from a rigorous mathematical proof based on some appropriate energy method. For the meantime, however, the results of this study clearly establish the need to re-examine this issue.

Acknowledgements

The authors are indebted to Dr. M. M. Rogers (NASA Ames) for his helpful comments and for allowing us to use unpublished results from his direct simulations on homogeneous shear flow. The support of P. S. Bernard through an ASEE/Navy Summer Faculty Research Fellowship at the Naval Research Laboratory, Washington, DC is also greatly appreciated.

References

[1]T. Von Karman, J. Aero. Sci. **4**, 131 (1937).

[2]A. A. Townsend, *The Structure of Turbulent Shear Flow* (Cambridge University Press, New York, 1956).

[3] J. O. Hinze, *Turbulence* (McGraw-Hill, New York, 1975).

[4]S. Corrsin, in *Handbuch der Physik VIII/2*, edited by S. Flugge & C. Truesdell (Springer, New York, 1963) p. 524.

[5]W. G. Rose, J. Fluid Mech. **25**, 97 (1966).

[6]F. H. Champagne, V. G. Harris and S. Corrsin, J. Fluid Mech. **41**, 81 (1970).

[7]V. G. Harris, J. A. Graham and S. Corrsin, J. Fluid Mech. **81**, 657 (1977).

[8]S. Tavoularis and S. Corrsin, J. Fluid Mech. **104**, 311 (1981).

[9]S. Tavoularis and U. Karnik, J. Fluid Mech. **204**, 457 (1989).

[10]J. J. Rohr, E. C. Itsweire, K. N. Helland and C. W. Van Atta, J. Fluid Mech. **187**, 1 (1988).

[11]R. S. Rogallo, NASA Technical Memorandum 81315 (1981).

[12]J. Bardina, J. H. Ferziger and W. C. Reynolds, *Stanford Univ. Report TF - 19* (1983).

[13]M. M. Rogers, P. Moin and W. C. Reynolds, *Stanford Univ. Report TF - 25* (1986).

[14]S. Tavoularis, Phys. Fluids **28**, 999 (1985).

[15]C. G. Speziale, and N. MacGiolla Mhuiris, J. Fluid Mech. **209**, 591 (1989).

[16]H. Tennekes and J. L. Lumley, *A First Course in Turbulence* (M. I. T. Press, Cambridge, MA, 1972).

[17]M. M. Rogers, *Private Communication* (1990).

[18]G. K. Batchelor and A. A. Townsend, Proc. R. Soc. London, Ser. A **193**, 539 (1947).

[19]G. Comte-Bellot and S. Corrsin, J. Fluid Mech. **48**, 273 (1971).

[20]M. Lesieur, *Turbulence in Fluids* (Martinus Nijhoff, Boston, 1987).

[21]A. Pumir and E. Siggia, Phys. Fluids A **2**, 220 (1990).

[22]S. S. Girimaji and S. B. Pope, Phys. Fluids A **2**, 242 (1990).

[23]C. G. Speziale, in *Forum on Turbulent Flows*, edited by W. W. Bower and M. J. Morris (ASME, New York, 1989), FED - Vol. 76, p. 19.

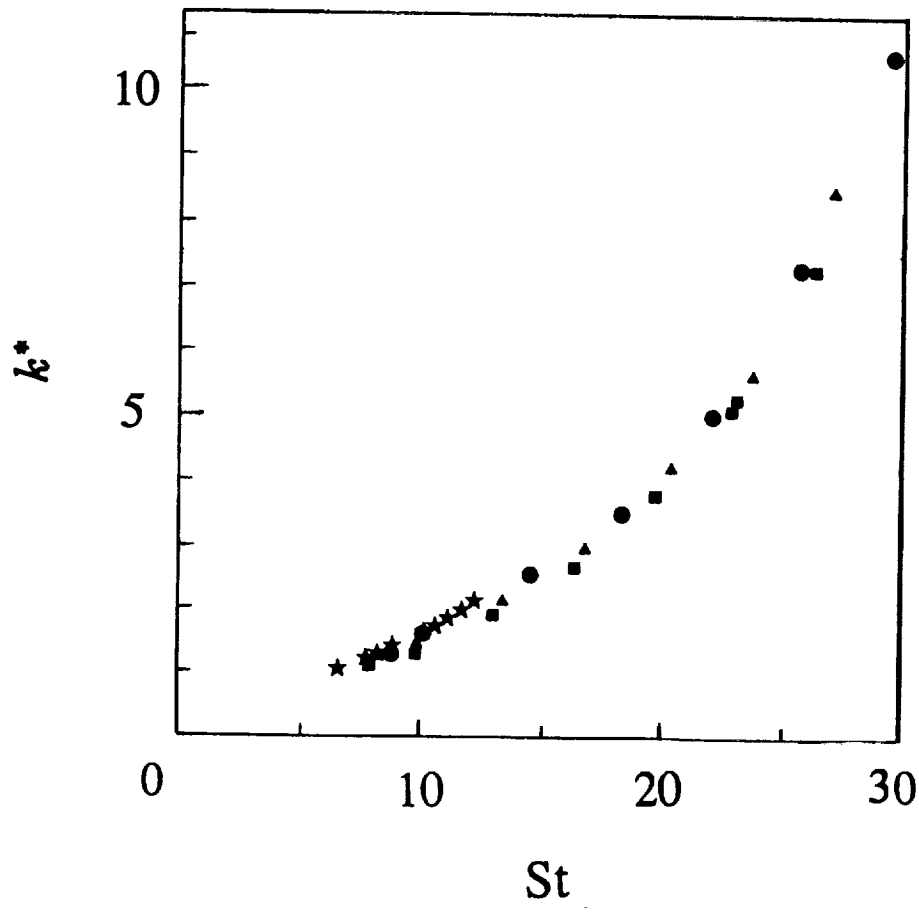

Figure 1. Experimental data on homogeneous shear flow measured by Tavoularis and Corrsin[8] and Tavoularis and Karnik[9] (as compiled by Rohr et al.[10]).

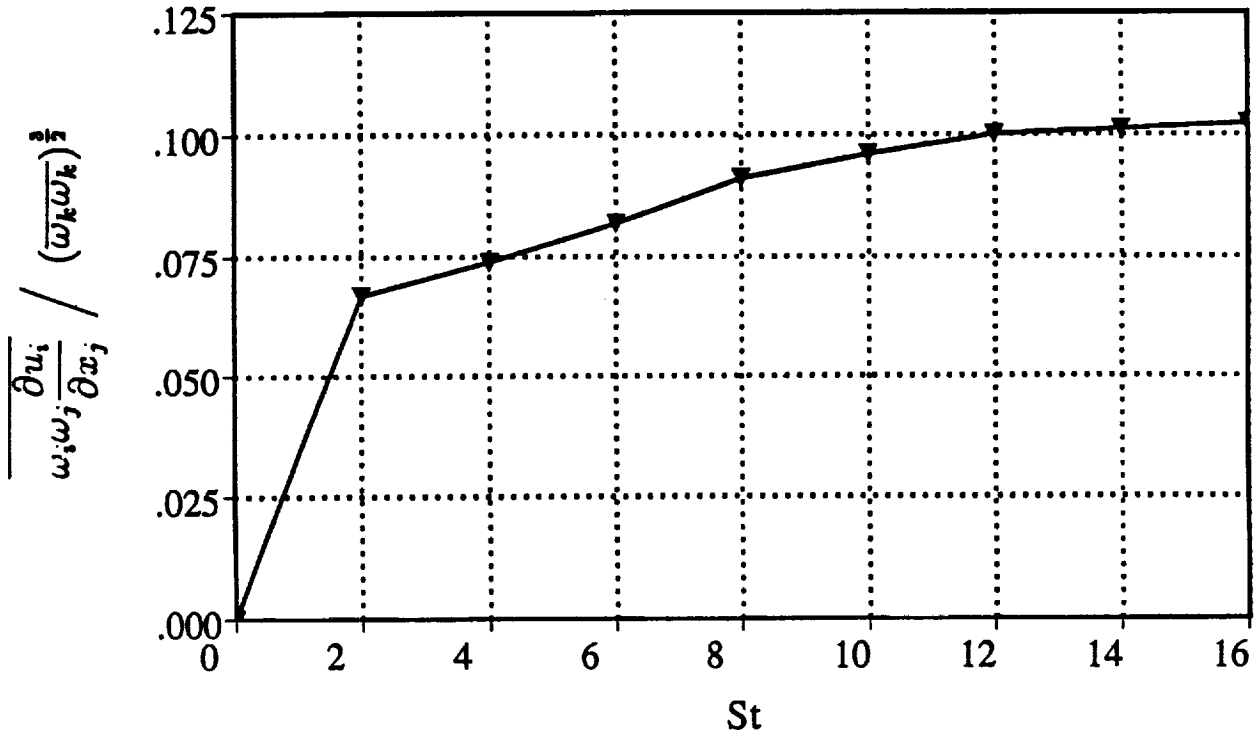

Figure 2. Time evolution of the normalized vortex stretching in homogeneous shear flow obtained from the direct numerical simulations of Rogers[17].

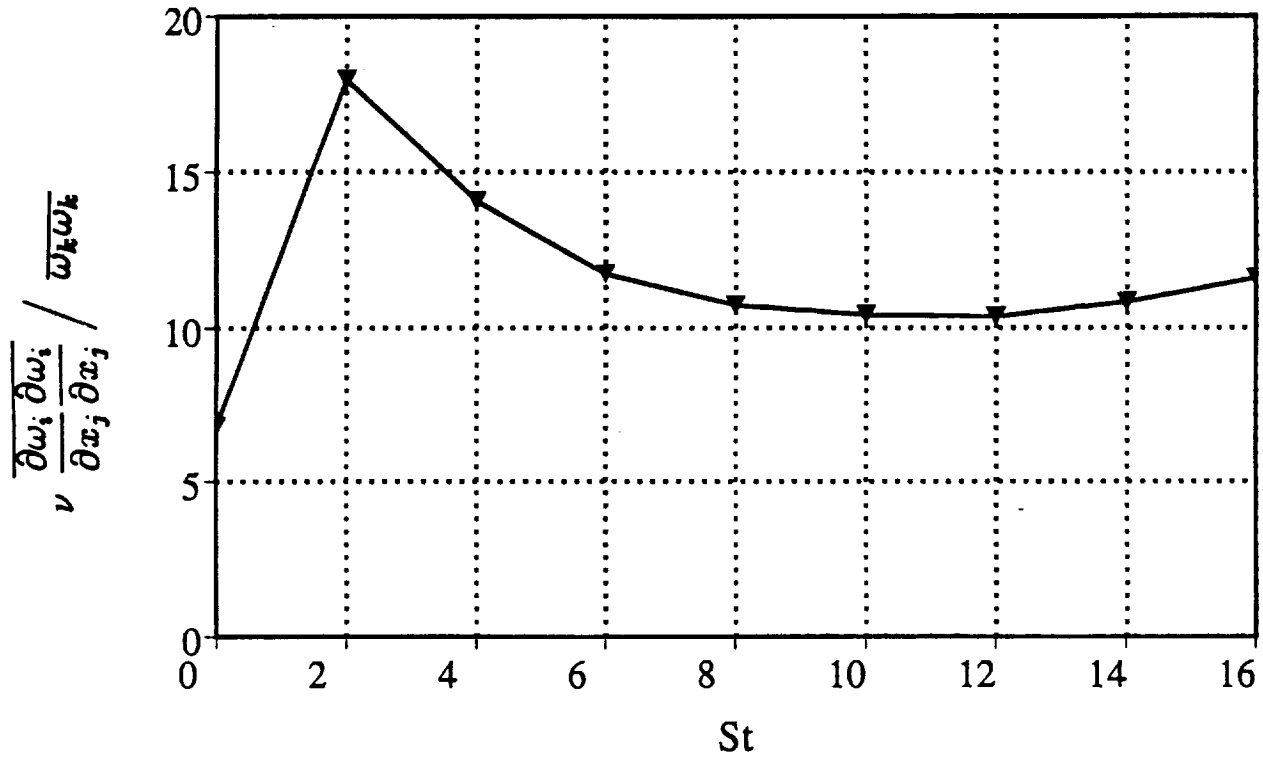

Figure 3. Time evolution of the ratio of the enstrophy destruction to the enstrophy in homogeneous shear flow obtained from the direct numerical simulations of Rogers[17].

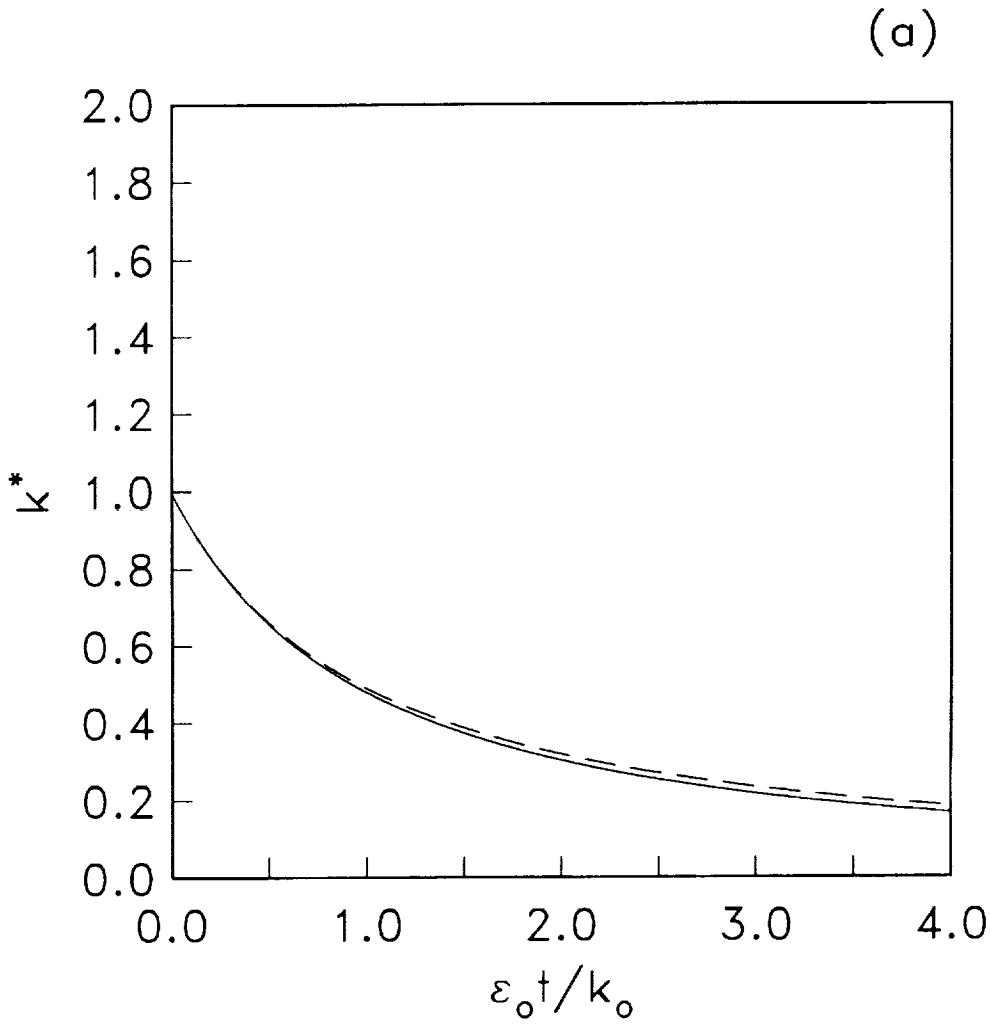

Figure 4. Comparison of solutions for isotropic decay: —— $S_K^{(0)} = 0.01$; - - - - standard $k - \epsilon$ model. (a) Time evolution of the turbulent kinetic energy for $R_{t_o} = 300$, and (b) time evolution of the enstrophy for $R_{t_o} = 10^6$.

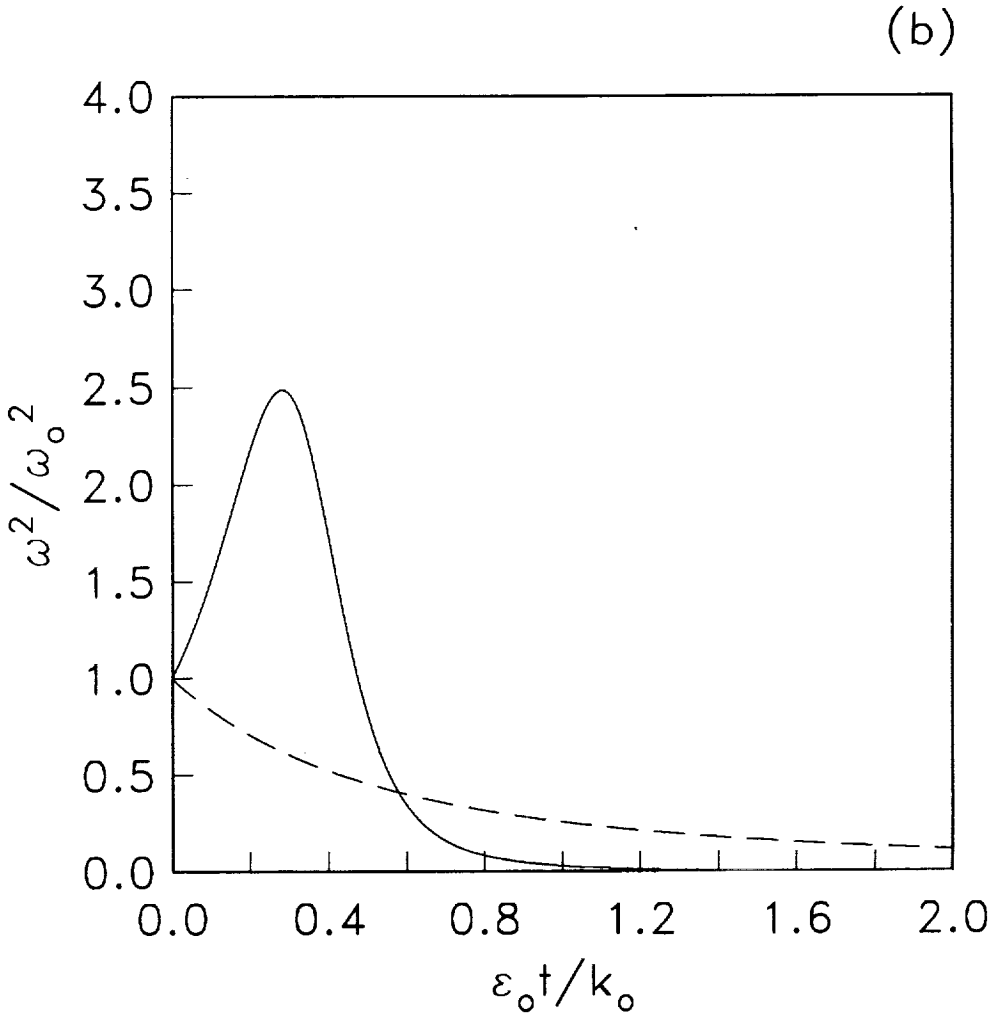

Figure 4. Comparison of solutions for isotropic decay: —— $S_K^{(0)} = 0.01$; - - - - standard $k - \epsilon$ model. (a) Time evolution of the turbulent kinetic energy for $R_{t_o} = 300$, and (b) time evolution of the enstrophy for $R_{t_o} = 10^6$.

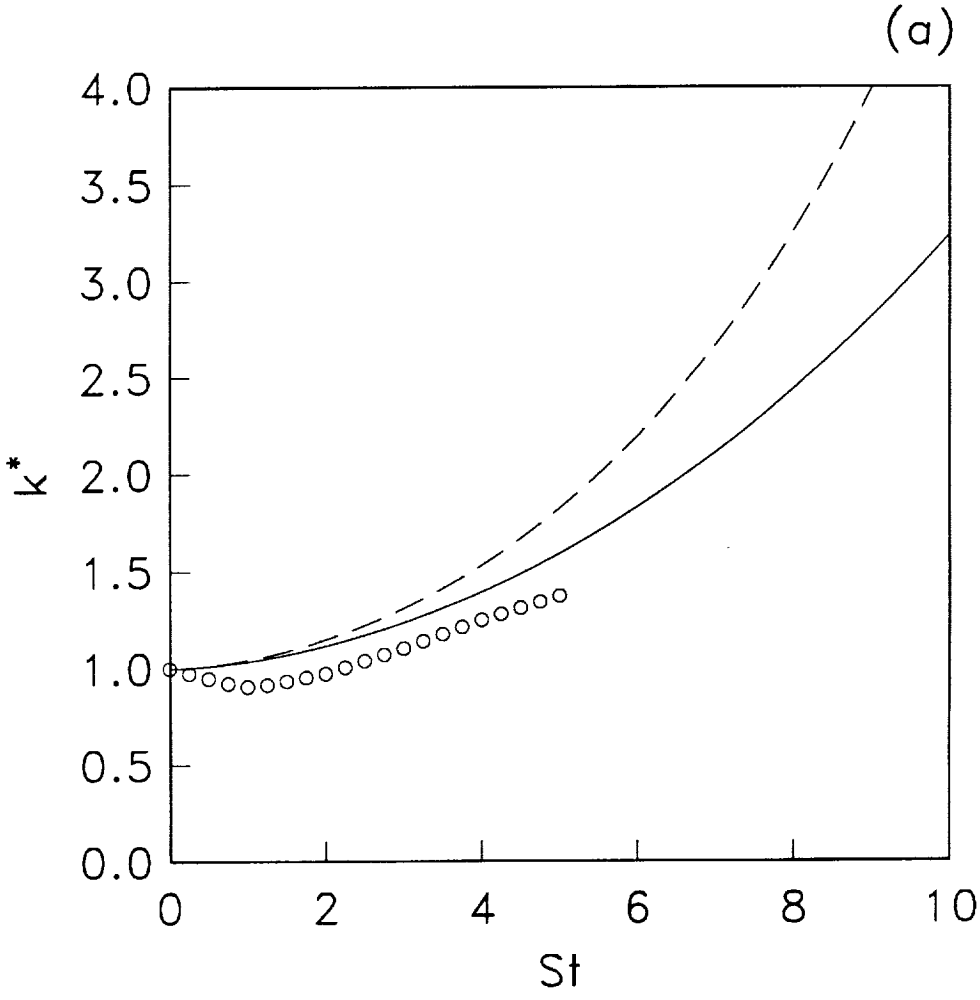

Figure 5. Comparison of the model predictions with the large-eddy simulations of Bardina, et al.[12]: o k^* from large eddy simulation[12]; —— k^* obtained with $S_K^{(0)} = 0.01$; - - - - k^* obtained from the standard $k - \epsilon$ model. (a) Short time solution, and (b) long time solution.

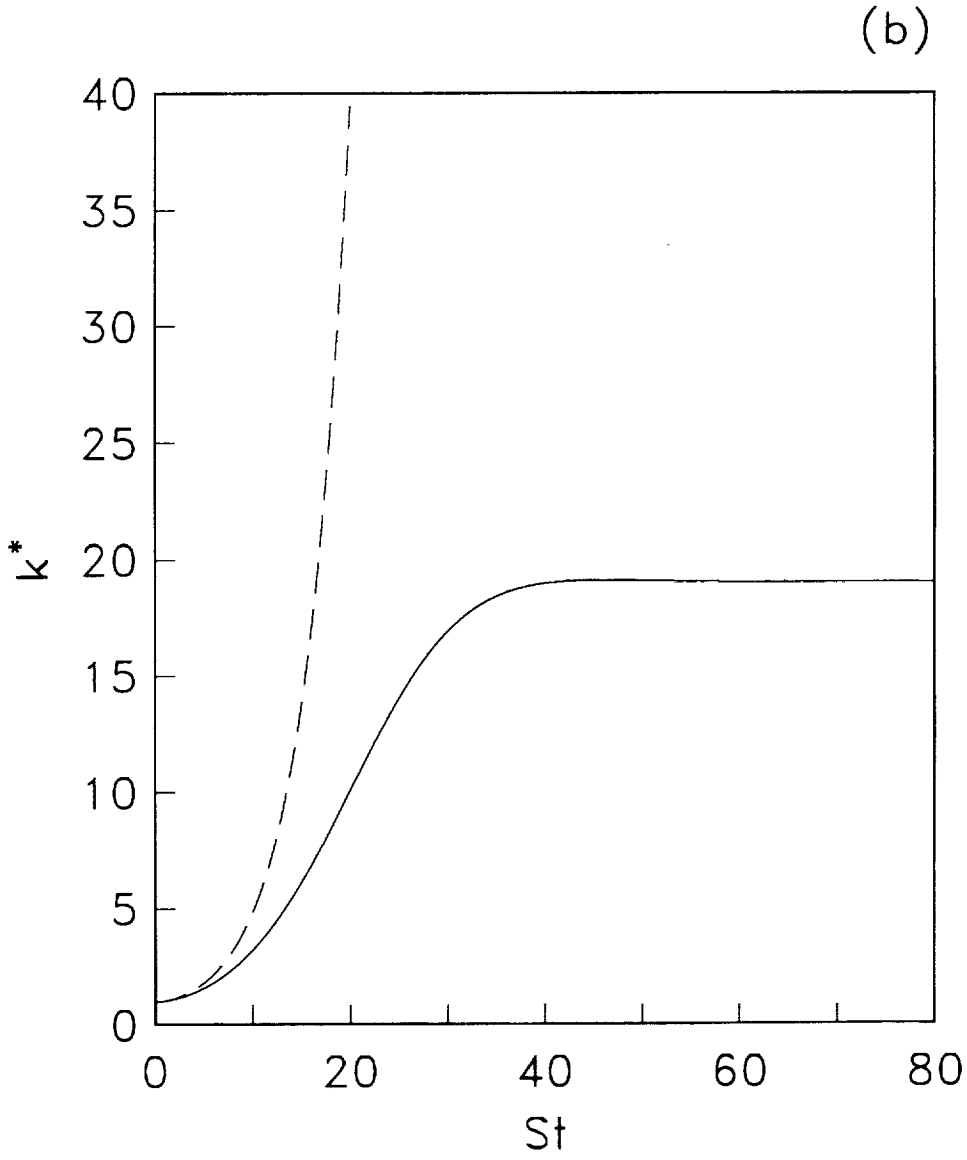

Figure 5. Comparison of the model predictions with the large-eddy simulations of Bardina, et al.[12]: o k^* from large eddy simulation[12]; —— k^* obtained with $S_K^{(0)} = 0.01$; - - - - k^* obtained from the standard $k - \epsilon$ model. (a) Short time solution, and (b) long time solution.

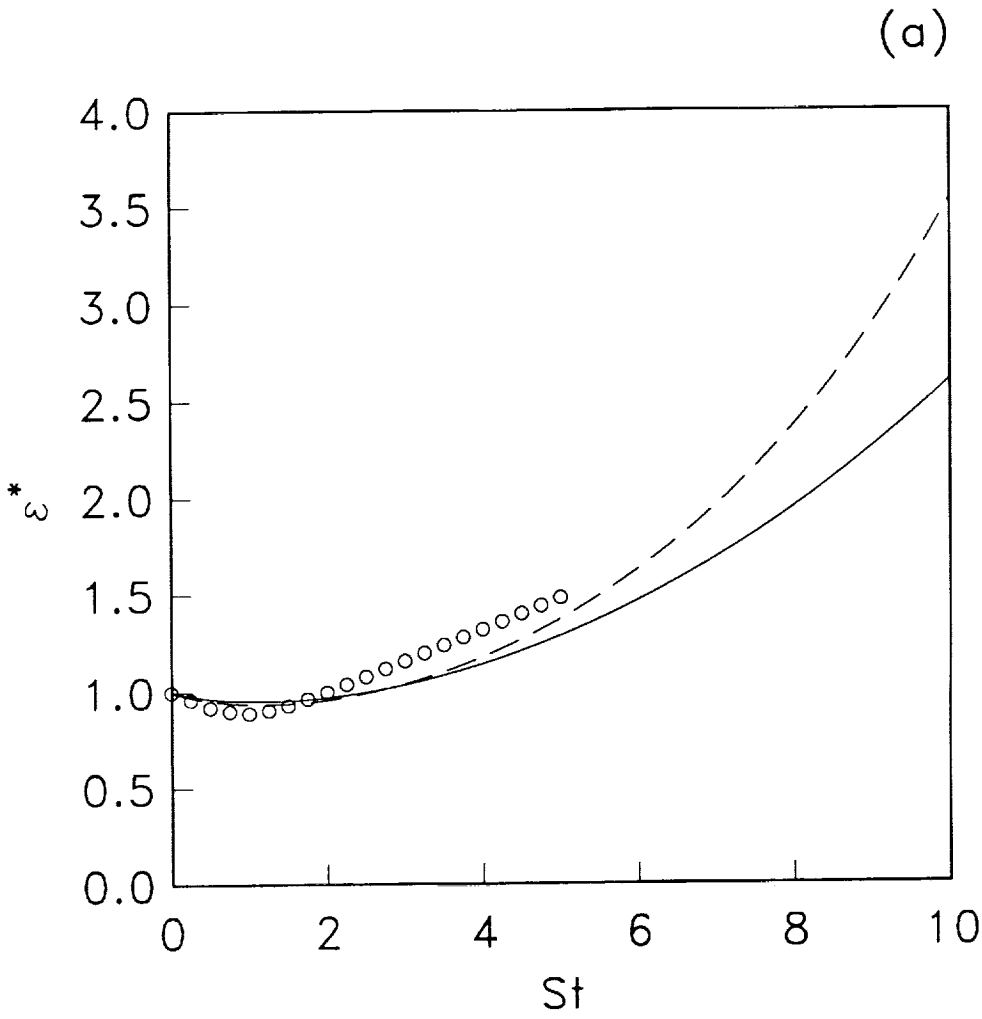

Figure 6. Comparison of the model predictions with the large-eddy simulations of Bardina, et al.[12]: o ϵ^* from large eddy simulation[12]; —— ϵ^* obtained with $S_K^{(0)} = 0.01$; - - - - ϵ^* obtained from the standard $k - \epsilon$ model. (a) Short time solution, and (b) long time solution.

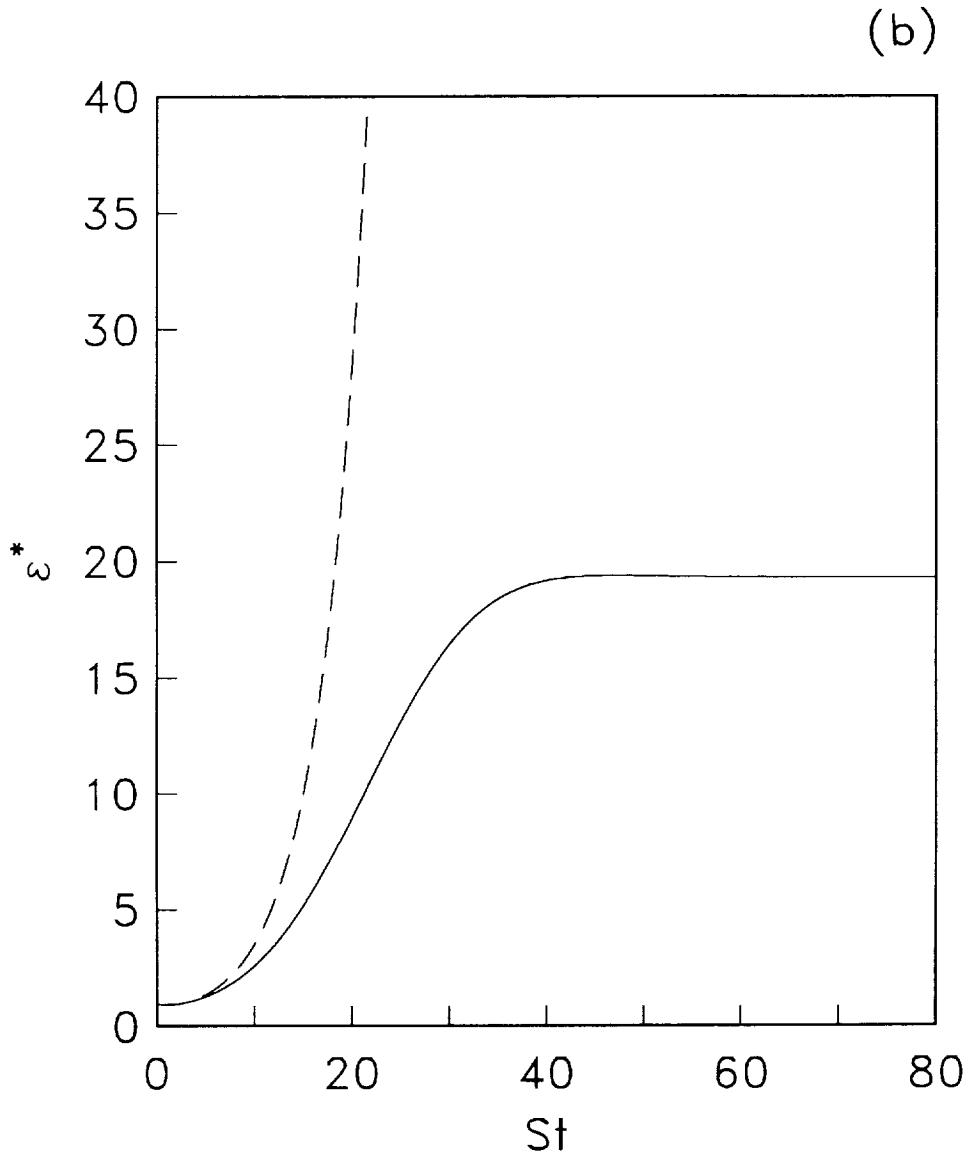

Figure 6. Comparison of the model predictions with the large-eddy simulations of Bardina, et al.[12]: o ϵ^* from large eddy simulation[12]; —— ϵ^* obtained with $S_K^{(0)} = 0.01$; - - - - ϵ^* obtained from the standard $k - \epsilon$ model. (a) Short time solution, and (b) long time solution.

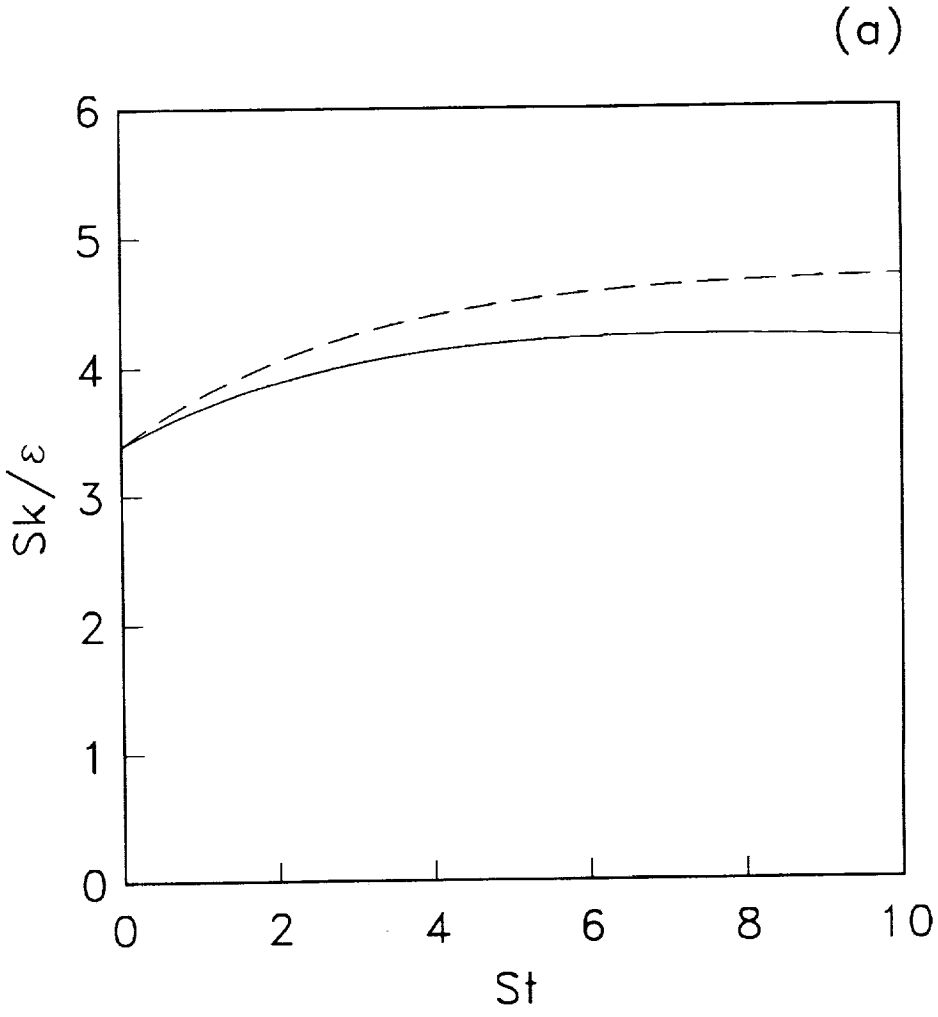

Figure 7. Comparison of the model predictions for Sk/ϵ: —— $S_K^{(0)} = 0.01$; - - - - standard $k-\epsilon$ model. (a) Short time solution, and (b) long time solution.

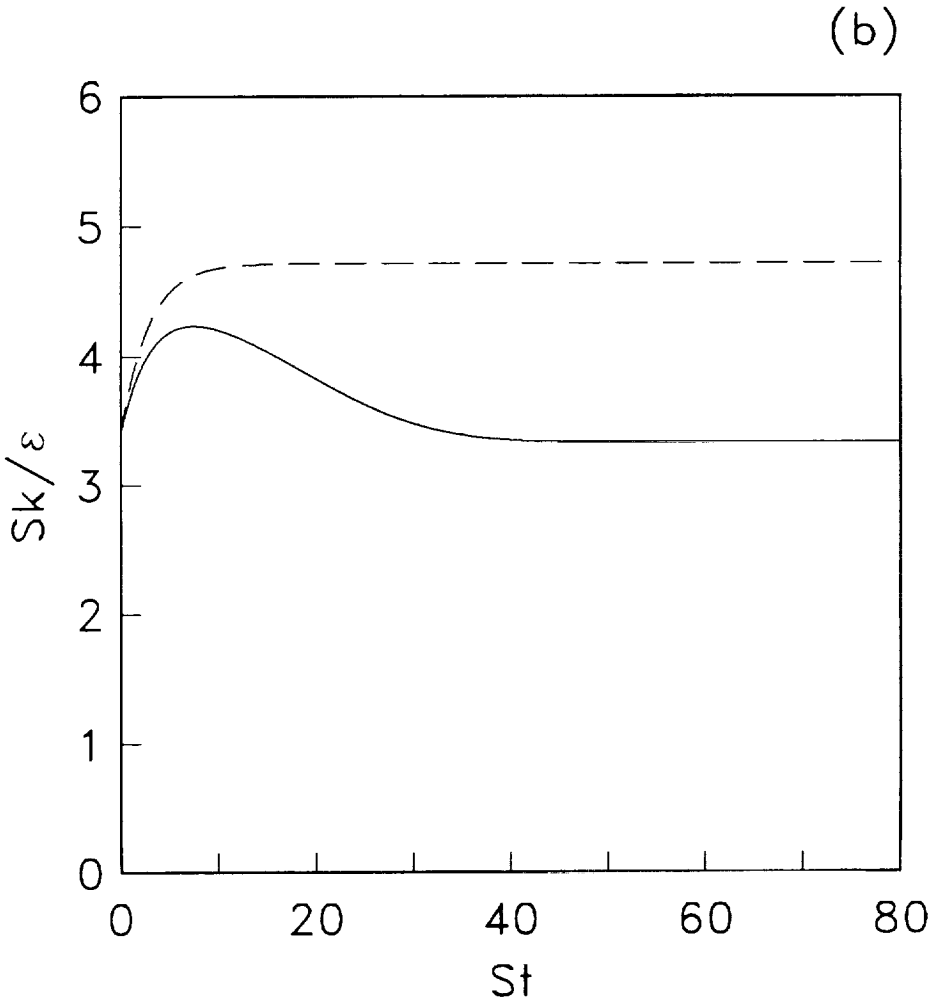

Figure 7. Comparison of the model predictions for Sk/ϵ: —— $S_K^{(0)} = 0.01$; - - - - standard $k - \epsilon$ model. (a) Short time solution, and (b) long time solution.

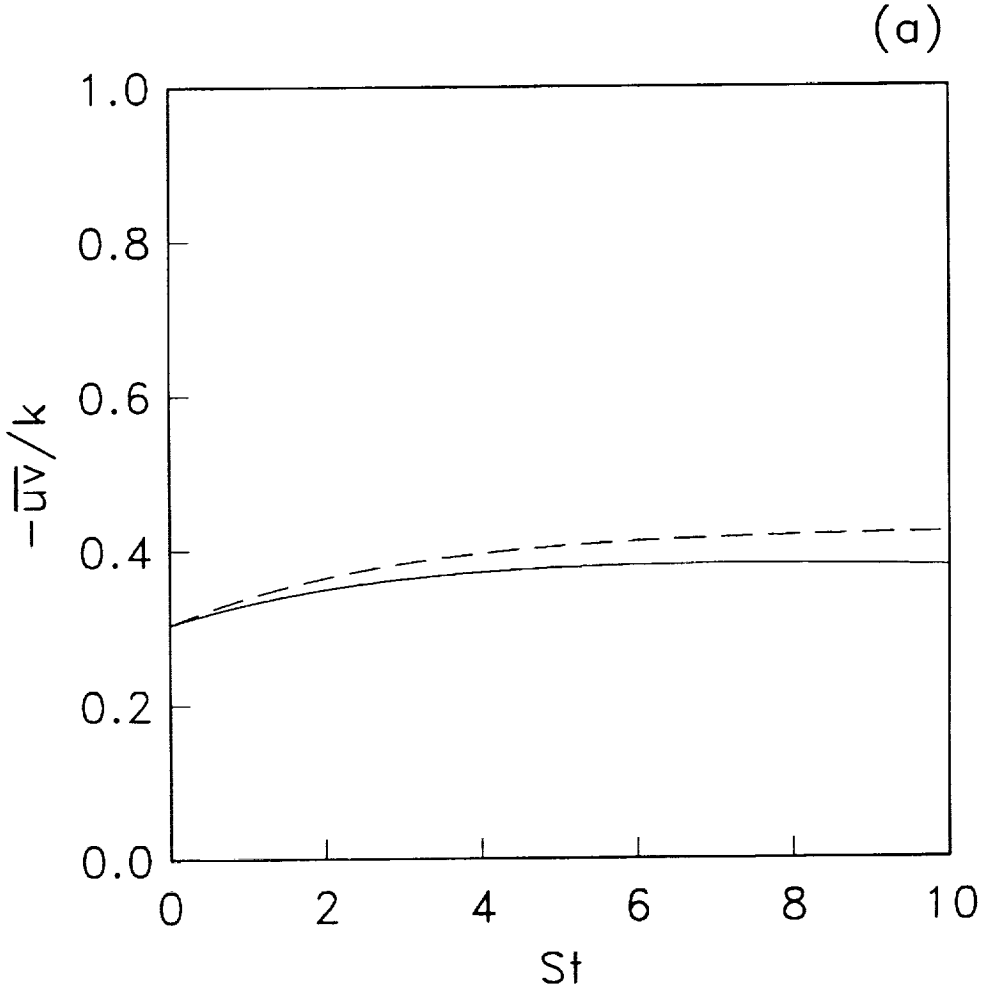

Figure 8. Comparison of the model predictions for $-\overline{uv}/k$: —— $S_K^{(0)} = 0.01$; - - - - standard $k-\epsilon$ model. (a) Short time solution, and (b) long time solution.

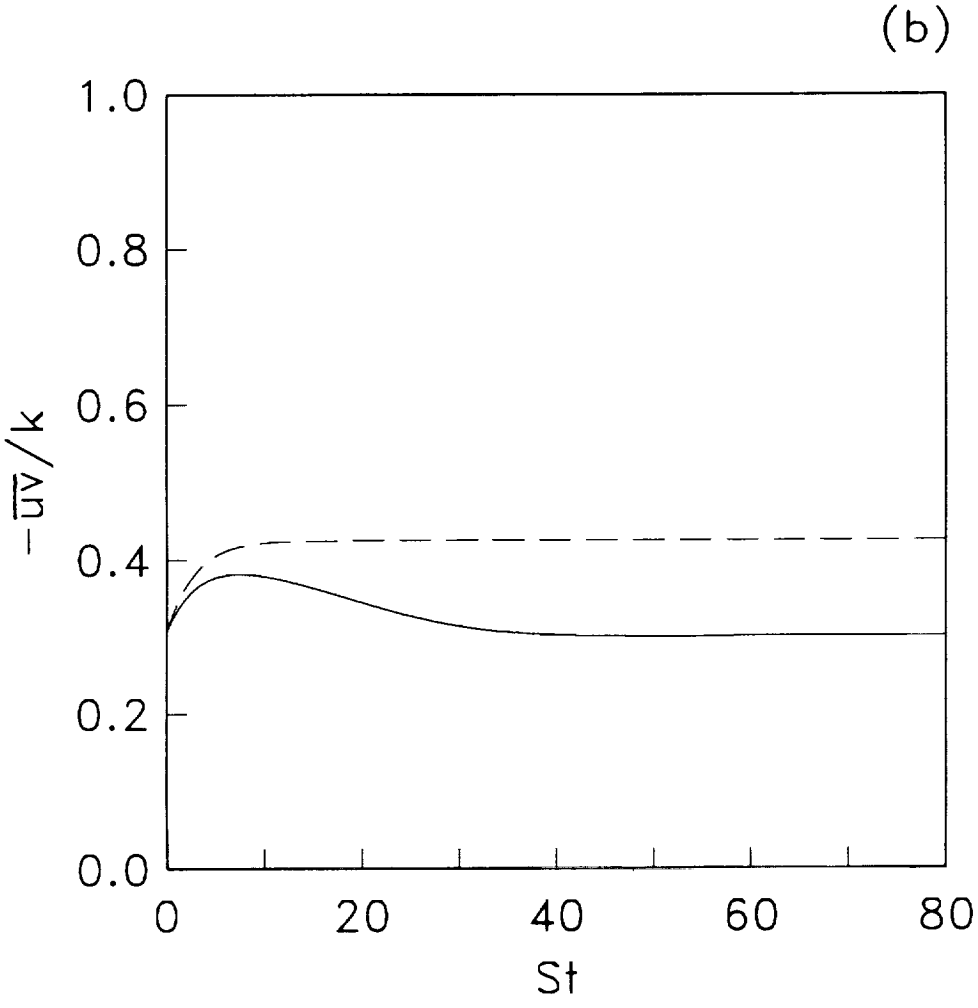

Figure 8. Comparison of the model predictions for $-\overline{uv}/k$: —— $S_K^{(0)} = 0.01$; - - - - standard $k - \epsilon$ model. (a) Short time solution, and (b) long time solution.

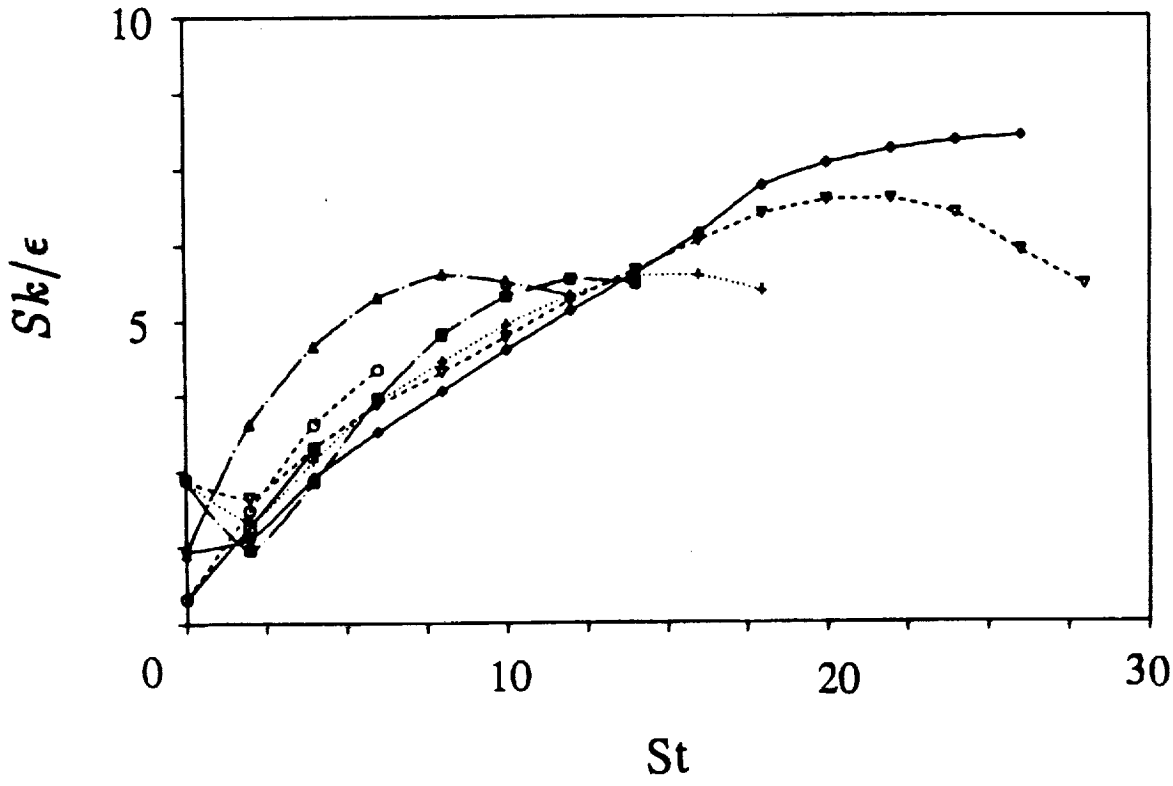

Figure 9. Time evolution of Sk/ϵ taken from the direct numerical simulation of Rogers et al.[13].

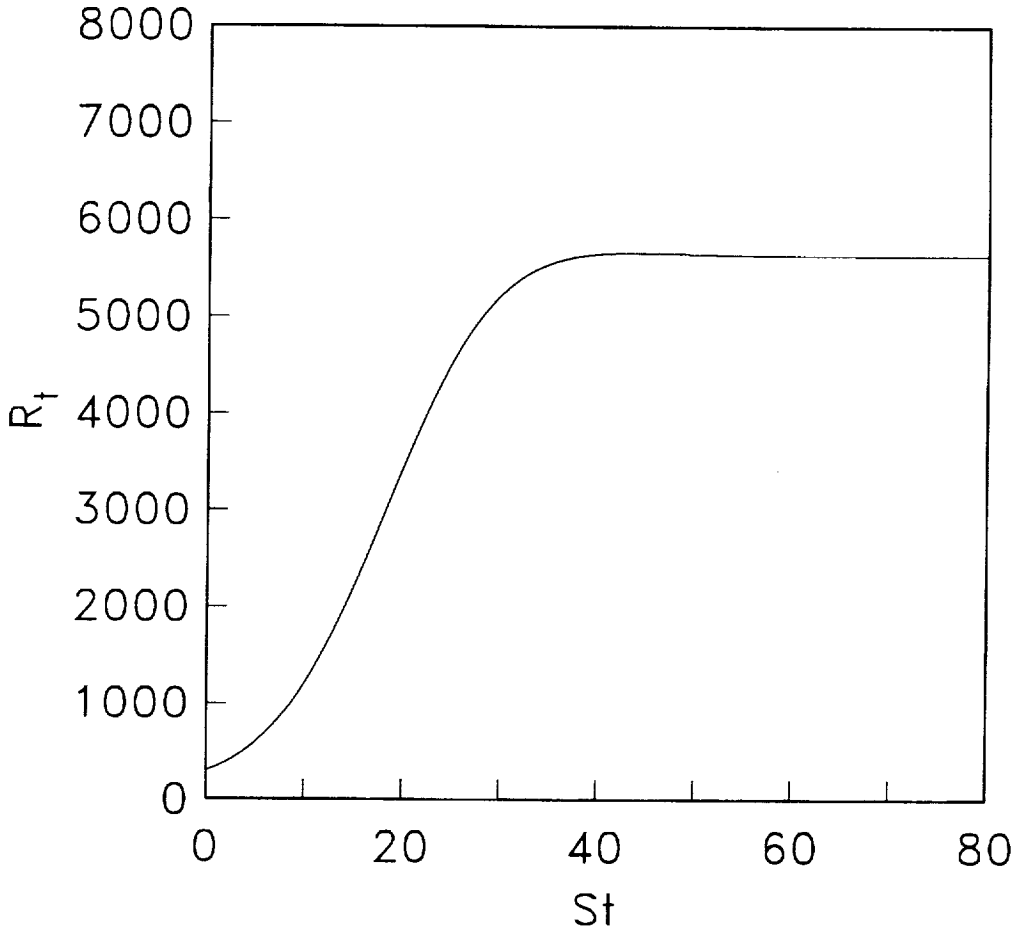

Figure 10. Time evolution of the turbulence Reynolds number R_t predicted by the $k-\epsilon$ model with vortex stretching.

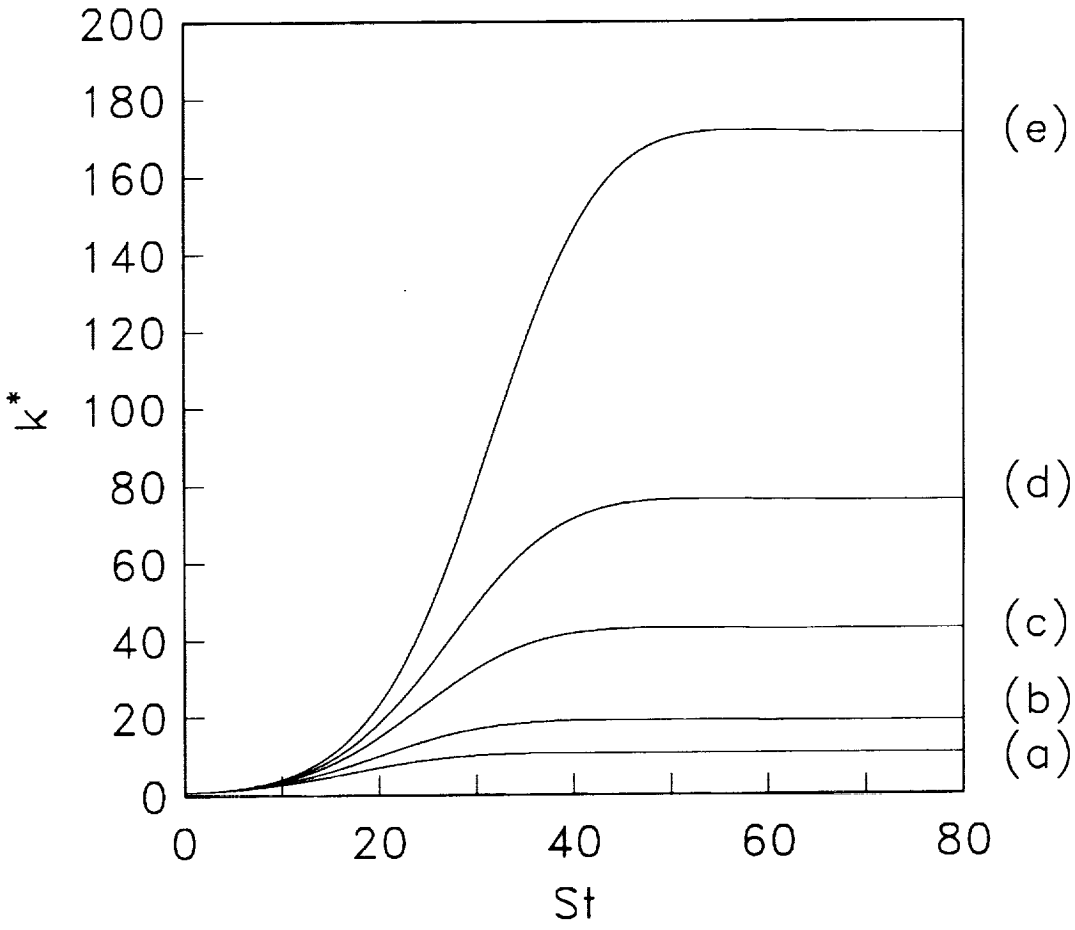

Figure 11. Sensitivity of the model predictions for the turbulent kinetic energy to $S_K^{(0)}$: (a) $S_K^{(0)} = 0.0133$; (b) $S_K^{(0)} = 0.01$; (c) $S_K^{(0)} = 0.0066$; (d) $S_K^{(0)} = 0.005$ and (e) $S_K^{(0)} = 0.0033$.

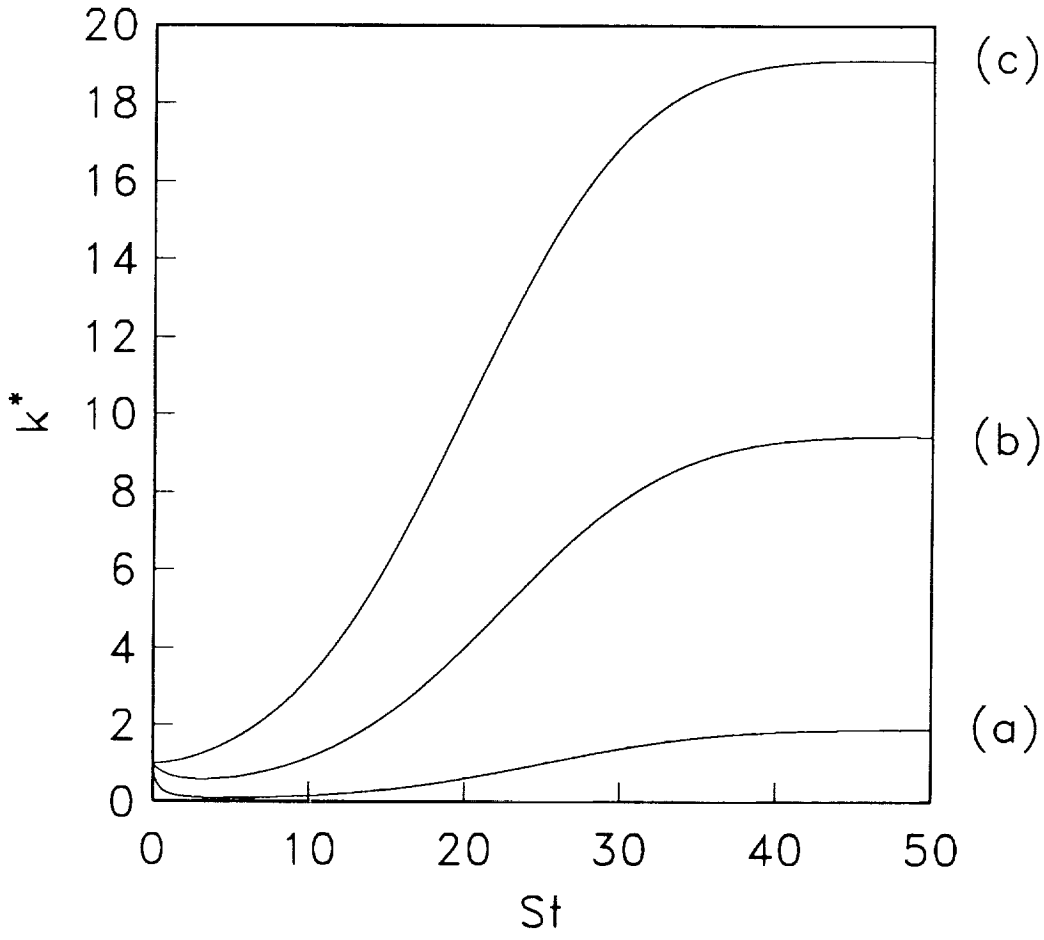

Figure 12. Sensitivity of the model predictions for the turbulent kinetic energy to ϵ_o/Sk_o: (a) $\epsilon_o/Sk_o = 3.0$; (b) $\epsilon_o/Sk_o = 0.6$ and (c) $\epsilon_o/Sk_o = 0.296$.

NASA
National Aeronautics and Space Administration

Report Documentation Page

1. Report No.	2. Government Accession No.	3. Recipient's Catalog No.
NASA CR-187439 ICASE Report No. 90-66		

4. Title and Subtitle

BOUNDED ENERGY STATES IN HOMOGENEOUS TURBULENT SHEAR FLOW -- AN ALTERNATIVE VIEW

5. Report Date
October 1990

6. Performing Organization Code

7. Author(s)

Peter S. Bernard
Charles G. Speziale

8. Performing Organization Report No.
90-66

10. Work Unit No.
505-90-21-01

9. Performing Organization Name and Address

Institute for Computer Applications in Science and Engineering
Mail Stop 132C, NASA Langley Research Center
Hampton, VA 23665-5225

11. Contract or Grant No.
NAS1-18605

13. Type of Report and Period Covered
Contractor Report

12. Sponsoring Agency Name and Address

National Aeronautics and Space Administration
Langley Research Center
Hampton, VA 23665-5225

14. Sponsoring Agency Code

15. Supplementary Notes

Langley Technical Monitor:
Richard W. Barnwell

To be submitted to Physics of Fluids A.

Final Report

16. Abstract

The equilibrium structure of homogeneous turbulent shear flow is investigated from a theoretical standpoint. Existing turbulence models, in apparent agreement with physical and numerical experiments, predict an unbounded exponential time growth of the turbulent kinetic energy and dissipation rate; only the anisotropy tensor and turbulent time scale reach a structural equilibrium. It is shown that if vortex stretching is accounted for in the dissipation rate transport equation, then there can exist equilibrium solutions, with bounded energy states, where the turbulence production is balanced by its dissipation. Illustrative calculations are presented for a k-ε model modified to account for vortex stretching. The calculations indicate an initial exponential time growth of the turbulent kinetic energy and dissipation rate for elapsed times that are as large as those considered in any of the previously conducted physical or numerical experiments on homogeneous shear flow. However, vortex stretching eventually takes over and forces a production-equals-dissipation equilibrium with bounded energy states. The validity of this result is further supported by an independent theoretical argument. It is concluded that the generally accepted structural equilbrium for homogeneous shear flow with unbounded component energies is in need of re-examination.

17. Key Words (Suggested by Author(s))	18. Distribution Statement
turbulence; homogeneous shear flow; vortex stretching; K-ε model	34 - Fluid Mechanics and Heat Transfer Unclassified - Unlimited

19. Security Classif. (of this report)	20. Security Classif. (of this page)	21. No. of pages	22. Price
Unclassified	Unclassified	35	A03